



Rapid Control Prototyping Platform for Real-Time Implementation of IM Speed Controllers

Mansour Bechar ^{1*}, Mohamed Habbab ¹, Younes Safi ¹

¹ Laboratory of CAOSEE, University of Tahri Mohammed Bechar, Algeria, bechar.mensour@univ-bechar.dz

*Corresponding author: (Mansour Bechar), *Email Address:* bechar.mensour@univ-bechar.dz

Abstract

In this paper, a rapid control prototyping platform for Real-Time implementation of IM speed controllers is made. The sliding mode controller, the nonlinear PI controller and the classical PI controller are applied to control an induction motor. All controllers were successfully implemented in real-time using rapid control prototyping techniques based on the digital simulator OP5600 that simulate the vector control of induction motor technique with the real speed sensor. The model first developed under Matlab/Simulink on RT-LAB software then loaded on the target via network connections TCP/IP protocol. Each response is analyzed and explained by graphics considering the performance at different speeds and the response to compensate changes in load. Experimental results demonstrate the high precision and the robustness of the sliding mode controller compared with the vector controller PI and NPI mainly in case of speed sense reverse and load changes.

Keywords: Rapid Control Prototyping; Induction Motor; PI Controller; Nonlinear PI Controller; Sliding Mode Controller; Digital Simulator (OP5600).

<https://doi.org/10.63070/jesc.2026.003>

Received 30 November 2025; Revised 19 January 2026; Accepted 26 January 2026.

Available online 31 January 2026.

Published by Islamic University of Madinah on behalf of *Islamic University Journal of Applied Sciences*. This is a free open access article under the Creative Attribution (CC.BY.4.0) license.

(<http://creativecommons.org/licenses/by/4.0/>).

1. Introduction

Induction Motor (IM) drives are used in several industrial applications due to their advantages of simple construction, less maintenance and reliability. The main advantage is that IM does not require any mechanical commutator, because of this they are maintenance free motors. These machines are highly non-linear and it requires complex speed control techniques. Different methods of speed control are developed and it can be classified into scalar and vector control methods. Scalar current control may be adequate for a simple low-performance drive system, but for high performance drive system it is not preferred. Vector control method is a well-known control technique, which uses the principle of stator current control of IM to get desired speed control. The torque and flux are controlled separately in the vector controlled induction motor drives [1].

A lot of speed controllers for induction motor have been proposed in the last few years. In our case we focused on three main control strategies:

First one, proportional integral (PI) controller [2]. PI controller can be easily implemented for second order system using analytic approach. In fact 3-phase induction motor system is accurately modelled as third order system without approximation [3, 4]. It is difficult to use the PI controller alone for third or higher order plant as the order of the plant is greater than the number of zeros provided by the PI controller [5, 6]. PI controller has the ability to control the speed of induction motor and also provide stability but, it does not come up with wide overshoot and large settling time.

Second one, a nonlinear PI (NPI) controller for speed sensorless control of the IM. While, the improvement of NPI controller is achieved by the use of nonlinear gains [7], the combination of nonlinear terms can provide additional degrees of freedom to achieve a much improved system performance. The NPI controller can adjust its gains in real time according to the speed error and it is able to reject the effect of time-varying and nonlinear behaviors in the process [8].

Third one, the sliding mode is an effective control strategy for nonlinear systems with uncertainties [9]. Its principle is based on the definition of a surface called sliding surface depending on system states so that it is attractive. The synthesized global control consists of two terms: the first allows the state trajectory to approach this surface and the second maintaining and sliding along it towards the origin of the phase plane [10]. It is characterized by good robustness, fast response time and disturbance rejection. However, the one of the drawbacks of this controller is the chattering phenomenon caused from the discontinuous control action.

In our paper, we present a comparative study between the cited controllers using a rapid control prototyping techniques (RCP). The sliding mode and the PI and nonlinear PI controllers are proposed.

This paper begins with the introduction of the speed control of an induction motor drive system with different types of control strategies. The following section explains the operation of the proposed field-oriented control techniques. The proposed techniques are implemented using (OP5600) RTDS, and the analysis of experimental results is discussed in section VI. The conclusion of this project is discussed in the last section.

2. Model of Induction Machine

The dynamic model of induction motor in two-phase stationary frame with assuming that the stator current and the flux as state variables. It is described as follows [11-12]:

$$\left\{ \begin{array}{l} \frac{di_{s\alpha}}{dt} = -\frac{1}{\sigma \cdot L_s} \left(R_s + \left(\frac{M_{sr}}{L_r} \right)^2 \cdot R_r \right) i_{s\alpha} + \frac{M_{sr} \cdot R_r}{\sigma \cdot L_s \cdot L_r^2} \varphi_{r\alpha} \\ \quad + \frac{M_{sr}}{\sigma \cdot L_s \cdot L_r} w_r \cdot \varphi_{r\beta} + \frac{1}{\sigma \cdot L_s} V_{s\alpha} \\ \frac{di_{s\beta}}{dt} = -\frac{1}{\sigma \cdot L_s} \left(R_s + \left(\frac{M_{sr}}{L_r} \right)^2 \cdot R_r \right) i_{s\beta} - \frac{M_{sr}}{\sigma \cdot L_s \cdot L_r} w_r \cdot \varphi_{r\alpha} \\ \quad + \frac{M_{sr} \cdot R_r}{\sigma \cdot L_s \cdot L_r^2} \varphi_{r\beta} + \frac{1}{\sigma \cdot L_s} V_{s\beta} \\ \frac{d\varphi_{r\alpha}}{dt} = \frac{M_{sr} \cdot R_r}{L_r} i_{s\alpha} - \frac{R_r}{L_r} \varphi_{r\alpha} - w_r \cdot \varphi_{r\beta} \\ \frac{d\varphi_{r\beta}}{dt} = \frac{M_{sr} \cdot R_r}{L_r} i_{s\beta} + w_r \cdot \varphi_{r\alpha} - \frac{R_r}{L_r} \varphi_{r\beta} \end{array} \right. \quad (1)$$

Where

$i_{s\alpha}$, $i_{s\beta}$ are stator current vector components in $[\alpha, \beta]$ stator coordinate system.

$V_{s\alpha}$, $V_{s\beta}$ are stator voltage vector components in $[\alpha, \beta]$ stator coordinate system.

$\varphi_{r\alpha}$, $\varphi_{r\beta}$ are rotor magnetic flux in $[\alpha, \beta]$ stator coordinate system.

M_{sr} Magnetizing inductance; L_r Rotor inductance; L_s Stator inductance; R_r Rotor resistance; R_s

Stator resistance; w_r Rotor angular speed; σ leakage coefficient $\sigma = 1 - \frac{M_{sr}^2}{L_r \cdot L_s}$; P poles number; $Tr = \frac{L_r}{R_r}$

the rotor time constant $\tau_r = 1 - \frac{M_{sr}^2}{L_r \cdot L_s}$.

The electromagnetic torque can be expressed by:

$$T_e = \frac{3.P.M_{sr}}{2.L_r} \cdot (\varphi_{r\alpha} \cdot i_{s\beta} - \varphi_{r\beta} \cdot i_{s\alpha})$$

3. Field Oriented Control of IM

The FOC has been developed to allow varying IM speed over a wide range. It separates the stator currents of IM into flux and torque components in the (d, q) coordinate reference frame. The model equation (1) is a heavily coupled, multivariable and nonlinear system. These properties complicate the control design of the IM. The rotor flux-oriented coordinate is applied in order to simplify the model of the IM, where the rotor flux is aligned to the direct axis (d) and the electromagnetic torque is aligned to the quadratic axis (q). In this coordinate system the rotor flux is assumed as [13]:

$$\begin{cases} \varphi_{rd} = \varphi_r \\ \varphi_{rq} = 0 \end{cases} \quad (2)$$

The electromagnetic torque expression becomes:

$$T_e = n_p \frac{M_{sr}}{L_r} \varphi_{rd} i_{qs} = K_t \cdot \varphi_{rd} \cdot i_{qs} \quad (3)$$

Where:

$$k_t = n_p \frac{M_{sr}}{L_r}$$

The new model motor dynamics is described by the following space vector differential equations:

$$\begin{cases} \frac{di_{ds}}{dt} = \frac{V_{ds}}{\sigma L_{sc}} - \eta_1 i_{ds} + n_p \omega i_{qs} - \left(\eta_2 i_{ds} + \alpha_1 \beta_1 \varphi_{rd} + \alpha_1 M_{sr} \frac{i_{qs}^2}{\varphi_{rd}} \right) \\ \frac{di_{qs}}{dt} = \frac{V_{qs}}{\sigma L_{sc}} - \eta_1 i_{qs} - n_p \omega i_{ds} - \beta_1 n_p \omega \varphi_{rd} - R_r \left(\eta_2 i_{qs} + \alpha_1 M_{sr} \frac{i_{qs} i_{ds}}{\varphi_{rd}} \right) \\ \frac{d\omega}{dt} = \mu \varphi_{rd} i_{qs} - \frac{T_l}{J} \\ \frac{d\varphi_{rd}}{dt} = \alpha_1 M_{sr} R_r i_{ds} - \alpha_1 R_r \varphi_{rd} \end{cases} \quad (4)$$

as:

$$\mu = \frac{2n_p M_{sr}}{2JL_r}; \eta_1 = \frac{R_s}{\sigma L_r}; \eta_2 = \frac{M_{sr}^2}{\sigma L_s L_r^2}; \alpha_1 = \frac{1}{L_r}; \beta_1 = \frac{M_{sr}}{\sigma L_s L_r}$$

Fig. 1, is shown the block diagram of field oriented control of IM with PI speed controller.

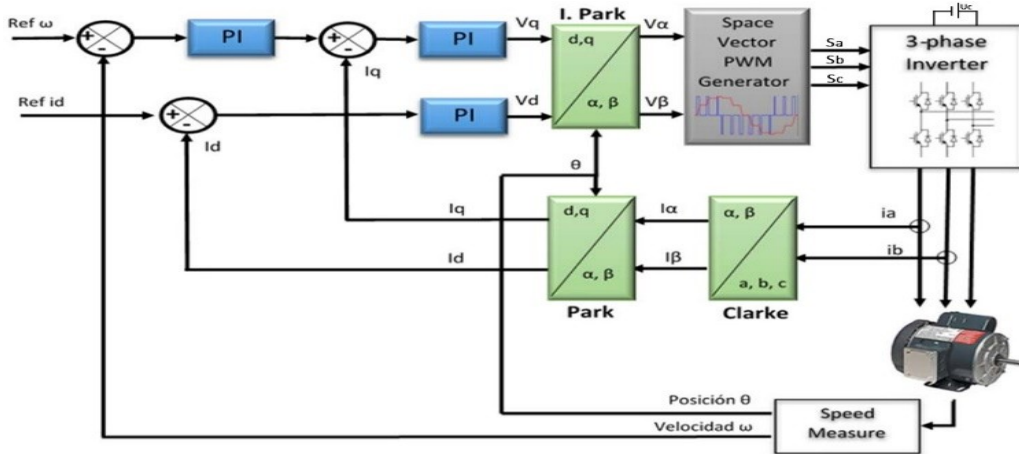


Figure 1. IM field oriented control.

4. Controller Synthesis

In this section, three types of controllers are examined and presented to regulate the speed of the IM.

4.1 Proportional integral (PI) controller

The conventional Proportional plus Integral controller (PI) is a simple speed controller in industrial applications. Under the load condition, the PI controllers try to modify the motor speed to attain the desired system speed. The output of the PI controller is a function of the speed error and the integral of error [14]:

$$u(t) = K_p e(t) + K_i \int e(t) d(t) \quad (5)$$

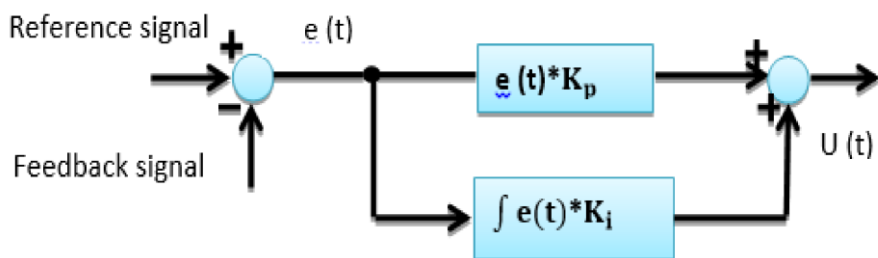


Figure 2. The block diagram of the used PI speed controller.

4.2 Non Linear (PI) Controller

In order to improve the control quality, a nonlinear PI (NPI) induction motor speed controller can be constructed as shown in Fig. 3, The combination of a nonlinear terms can provide additional degrees of freedom to achieve a much improved system performance. The nonlinear PI controller action is given by [15].

$$T_e^* = K_p \cdot fal(e, \alpha_p, \delta_p) + K_i \cdot fal(\int e, \alpha_i, \delta_i) \quad (6)$$

$$fal(x, \alpha, \delta) = \begin{cases} |x|^\alpha \operatorname{sign}(x) & |x| > \delta, \delta > 0 \\ \frac{x}{\delta^{1-\alpha}} & |x| \leq \delta \end{cases} \quad (7)$$

Where

$fal(x, \alpha, \delta)$ is nonlinear function represented in Fig. 4,

x is a variable which can be e or $\int e \cdot dt$,

e is the error between the speed reference and real speed of the induction motor $e = \omega_r^* - \omega_r$.

K_p and K_i are respectively proportional and integral gains of the PI controller.

T_e^* is the referential torque (the control signal), the parameters α_p and α_i are constant, empirically chosen in the range 0 to 1. When $\alpha_p = \alpha_i = 1$, the controller becomes a linear PI controller, δ is a constant, which can be set empirically to a small value.

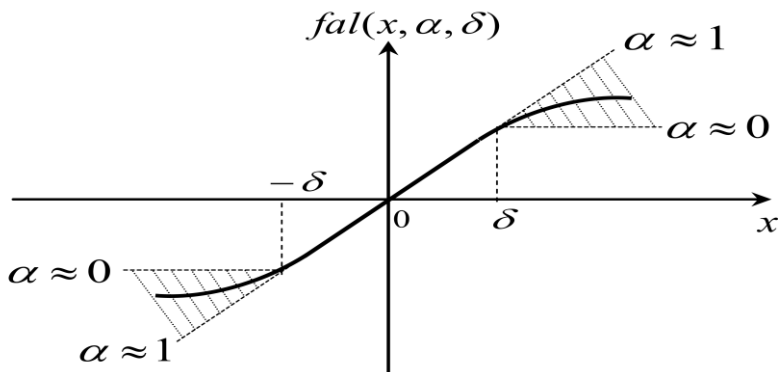


Figure 3. Function characteristics.

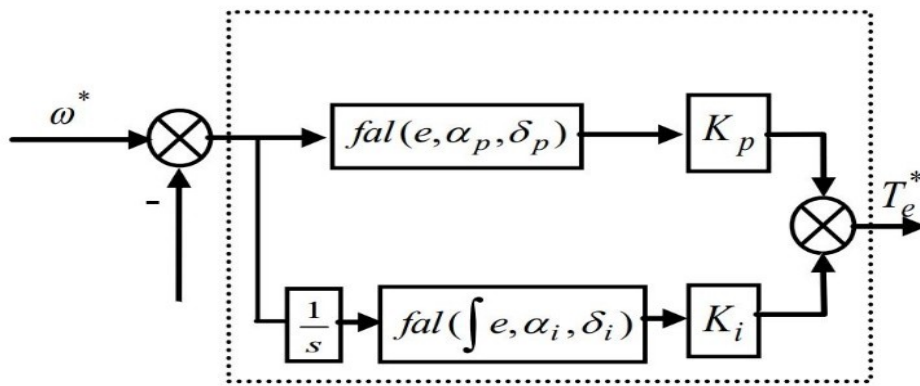


Figure. 4. Nonlinear PI controller.

4.3 Sliding Mode Controller Design

Based on complete indirect field orientation, sliding mode control with integral sliding surface is discussed in this section. Under the complete field oriented control, the mechanical equation can be equivalently described as:

$$J \frac{d\omega}{dt} + B\omega + T_l = T_e \quad (8)$$

The electromechanical equation can be modified as

$$\dot{\omega} + a\omega + d = bT_e \quad (9)$$

Where $a = \frac{B}{J}$, $b = \frac{1}{J}$ and $d = \frac{T_l}{J}$

By considering (9) with uncertainties as

$$\dot{\omega} = -(a + \Delta a)\omega - (d + \Delta d) + (b + \Delta b)T_e \quad (10)$$

Δa , Δb and Δd represents the uncertainties of the terms a , b and d introduced by system parameters J and B . Now let us define the tracking speed error further as

$$e(t) = \omega(t) - \omega^*(t) \quad (11)$$

Where ω^* is the rotor reference speed command in angularfrequency.

Taking derivative of (11) with respect to time yields

$$\dot{e}(t) = \dot{\omega}(t) - \dot{\omega}^*(t) = -ae(t) + f(t) + x(t) \quad (12)$$

Where the following terms have been collected in the signal $f(t)$,

$$f(t) = bT_e(t) - a\omega^* - d(t) - \dot{\omega}(t) \quad (13)$$

And the $x(t)$, lumped uncertainty, defined as

$$x(t) = -\Delta\alpha \omega(t) - \Delta d(t) + \Delta b T_e(t) \quad (14)$$

Now, the sliding variable with integral component, is defined as

$$S(t) = e(t) - \int_0^t (h - \alpha) e(\tau) d\tau \quad (15)$$

where h is a constant gain. Also in order to obtain the speed trajectory tracking, the following assumptions are made [16].

Assumption-1: The h must be chosen so that the term $(h - \alpha)$ is strictly negative and hence $h < 0$.

Then the sliding surface is defined as follows:

$$S(t) = e(t) - \int_0^t (h - \alpha) e(\tau) d\tau = 0 \quad (16)$$

Based on the developed switching surface, a switching control that guarantees the existence of sliding mode, a speed controller is defined as

$$f(t) = h e(t) - \beta \operatorname{sgn}(S(t)) \quad (17)$$

where β is the switching gain, $S(t)$ is the sliding variable defined by (15) and $\operatorname{sgn}(\cdot)$ is the sign function defined as

$$\operatorname{sgn}(S(t)) = \begin{cases} +1, & \text{if } S(t) > 0 \\ -1, & \text{if } S(t) < 0 \end{cases} \quad (18)$$

Assumption-2: The β must be chosen so that

$\beta \geq |x(t)|$ for all time. When the sliding mode occurs on the sliding surface (16), then, $S(t) = \dot{S}(t) = 0$ and the tracking error $e(t)$ converges to zero exponentially. Finally, the reference torque command T_e^* can be obtained by substituting (17) in (13) as follows.

$$T_e^*(t) = \frac{1}{b} \left[(h \cdot e) - \beta \operatorname{sgn}(S) + \alpha \omega^* + \dot{\omega}^* + d \right] \quad (19)$$

5. Experimental Results

Rapid control prototyping platform for validation of the proposed study between different controllers is shown in Fig. 5, this platform was built using RT-LAB as a real-time platform, and it contains OP-5600 OPAL-RT real-time simulator used as a core of the hardware prototype system. Currently, CAOSEE laboratory at Bechar university is equipped with one OP5600 OPAL-RT simulator and one drivelab OPAL-RT board [17]. The vector control algorithm is created in Matlab/Simulink software on the RT-LAB host computer with two subsystems SM and SC, the SM subsystem is converted into 'C' source code using Mathworks code generator Real-Time-Workshop (RTW) and compiled

using RT-LAB. This code is then uploaded into the OP5600 target via network connections TCP/IP protocol.

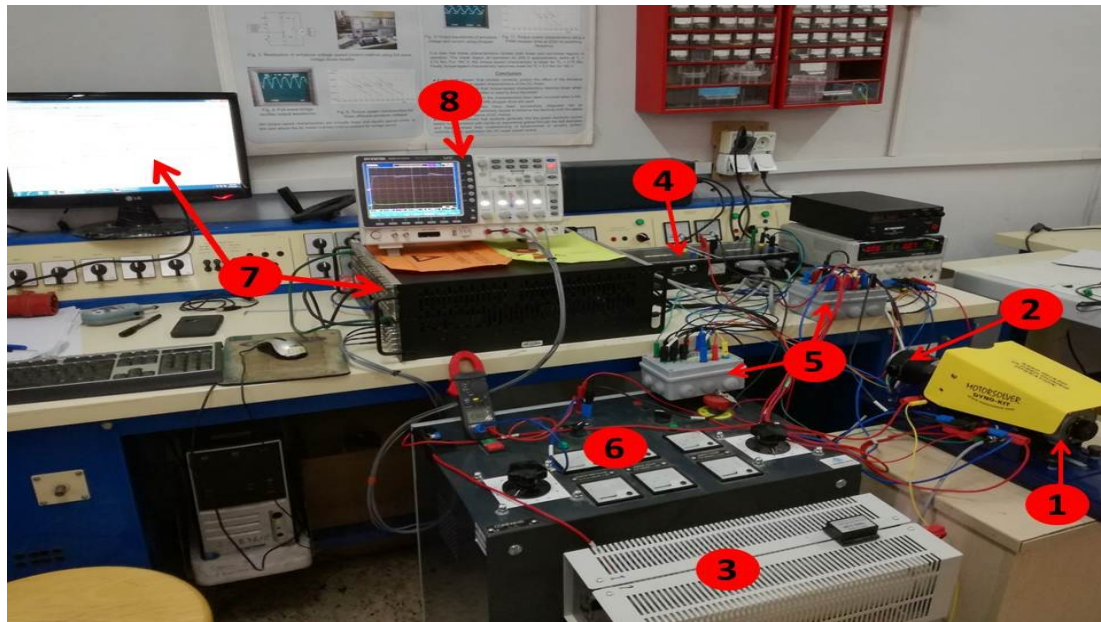


Figure 5. Rapid control prototyping system: real view of bench.

The test bench of RCP is shown in Fig. 5, that is composed of:

- (1) Squirrel cage induction motor with the following characteristics: Δ connected, four poles, 125 W, 4000 rpm, 30 V, 133 Hz with the 1024 points integrated incremental coder,
- (2) DC generator motor,
- (3) Resistive load,
- (4) Inverter Drivelab Board,
- (5) Hall type current sensors, voltage sensors,
- (6) Auto transformer (0-450 V),
- (7) OP5600 real-time digital simulator with Host computer equipped by RT-LAB software,
- (8) Numerical oscilloscope.

The different waveforms below show the experimental validation of field-oriented control in different operation modes such as transient and steady state, load application, reverse speed test, for the PI, NPI, and SMC controllers.

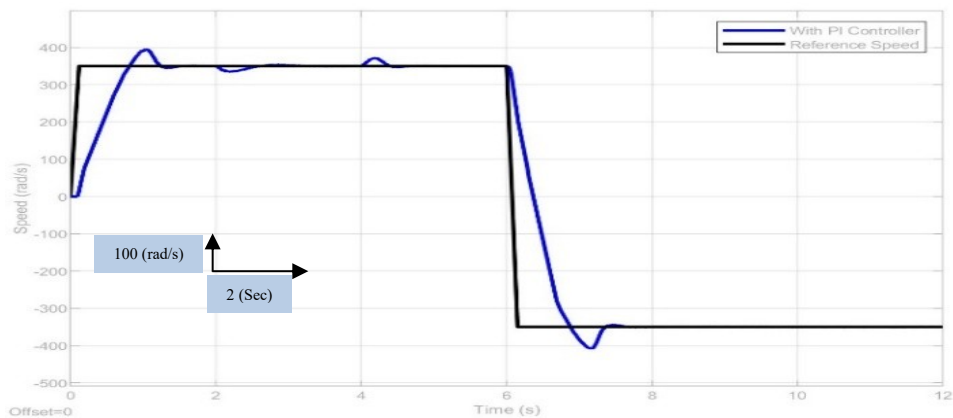


Figure 6. Rotor speed with PI controller.

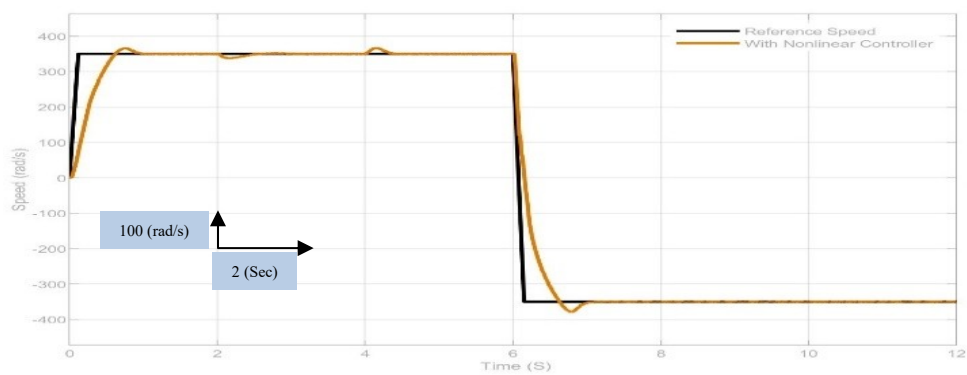


Figure 7. Rotor speed with nonlinear PI controller.



Figure 8. Rotor speed with SMC.

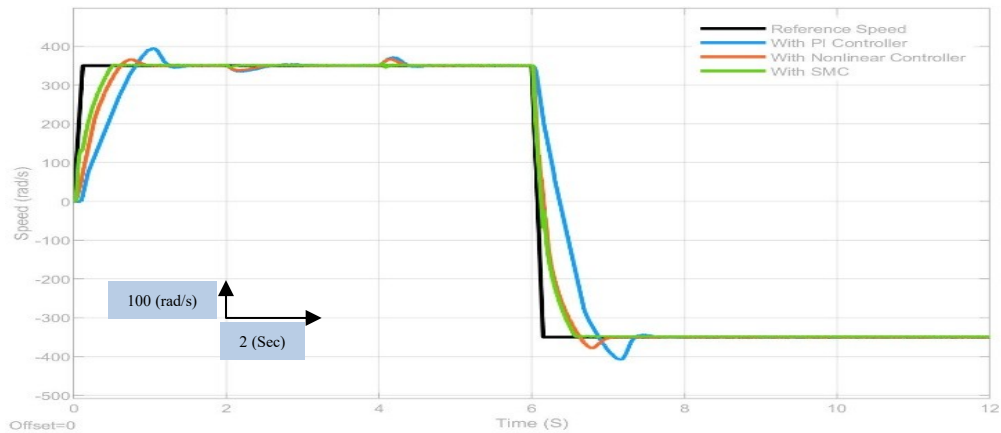


Figure 9. Rotor speeds with different controllers.

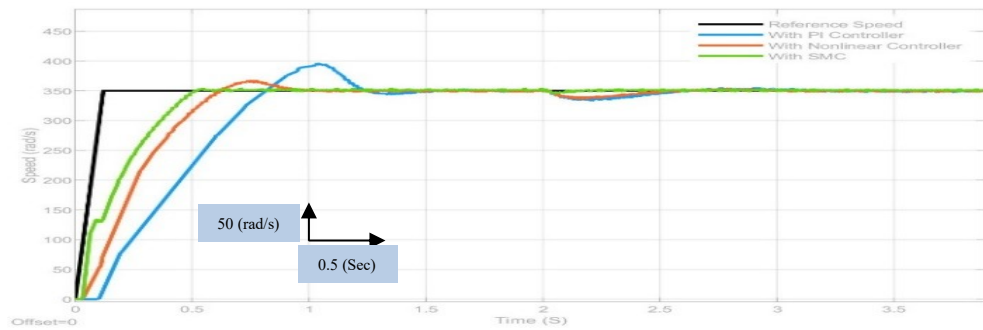


Figure 10. Zoom of rotor speeds.

First, the motor is started under no load with a nominal speed of 350rad/sec, and after 2 sec, a rated load is applied, in 4 sec the motor is unloaded again, at $t=6$ sec the speed sense reverses (350rad/sec, -350rad/sec).

Fig. 6 shows the behavior of an induction motor at nominal speed with a disturbance load application. The reference speed is set to 350rad/sec. It is clear that the PI controller exhibits good performances at steady state, but in the dynamic regime, when the motor starts up, the PI controller exceeds the saturation value and generates inadequate performances for the system as a large overshoot and a long settling time, as shown in Fig. 6.

In Fig. 7, the nonlinear PI controller rejects the load disturbance very rapidly compared with the PI controller, Fig. 7, rotor speed sense reversing (350rad/sec, -350rad/sec) the nonlinear PI provides perfect superposition and better tracking than PI by reducing the overshoot and settling time.

Fig. 8, shows the speed response of the SMC. The speed response of SMC has a small overshoot, and it is clear that the load change does not extend the proposed control performance. The system maintains robustness against the effects of the load change.

Based on comparative results obtained in Fig.9, it can be seen that the SMC can provide robust performance. It has been shown that the proposed control scheme performs reasonably well in practice, and that the speed tracking objective is achieved under speed step variations and load disturbances. The result for Fig.10, shows the zoomed performance of the rotor speed.

6. Conclusion

This work presents a comparative study between different controllers using a rapid control prototyping technique: the proportional integral (PI) controller, nonlinear PI controller and sliding mode controller. Controller tests were performed in order to make a comparison in Induction Machine speed performances.

Two different control strategies have been implemented. To obtain better performances than the PI classical speed controller, according to our real-time implementation, the sliding mode controller rejects perfectly the disturbances and the nonlinear PI controller is characterized by a small response time. Through the experimental results, the sliding mode and the nonlinear PI controllers present the high performances in speed tracking and disturbance rejection.

References

- [1] R. Krishnan, "ELECTRIC MOTOR DRIVES Modelling, Analysis and control", 1st Edition, Prentice-Hall, 2001.
- [2] S. Jung, and R.C. Dorf, "Novel analytic technique for PID and PIDA controller design", in Proc. 13th IFAC World Congress, San Francisco, USA, 1996.
- [3] R.C. Dorf and R.H. Bishop, "Modern Control System", 7th edition, Addison Wesley, 1995.
- [4] K. Ogata, "Modern Control Engineering", 2nd edition, Prentice Hall, 1990.
- [5] S. Jung and R.C. Dorf, "Analytic PIDA Controller Design Technique for a Third Order System", Proceedings of the 35th IEEE Conference on Decision and Control, Kobe, pp. 2513-2518, 11-13 December 1996.
- [6] R .C. Dorf and D. R. Miller, "A method for enhanced PID controller design", Journal of Robotics and Automation, vol.6, pp. 41 47, 1991.
- [7] Cruz, M. A. Gallegos, R. Alvarez, and F. Pazos, "Comparison of several nonlinear controllers for induction motors", IEEE Int'l. Power Electronics Congress (CIEP), 2004, pp. 134 –139.
- [8] Y.X. Su, Dong Sun, B.Y. Duan, "Design of an Enhanced Nonlinear PID Controller", Mechatronics 15 (2005) pp. 1005–1024.
- [9] Zhifeng Zhang, Jianguang Zhu, Renyuan Tang, Baodong Bai, and Hongyang Zhang, "Second order sliding mode control of flux and torque for induction motor", Power and Energy Engineering Conference (APPEEC), 2010 Asia-Pacific. IEEE, pp. 1-4, 2010.
- [10] M. Moutchou, A. Abbou, and H. Mahmoudi, "Induction machine speed and flux control using vector-sliding mode control with rotor resistance adaptation", International Review of Automatic Control, (Theory and Application) (IREACO), Vol. 5 (n. 6), 2012.

- [11] G. Tarchala, T. Orlowska-Kowalska, "Sliding mode speed observer for the induction motor drive with different sign function approximation forms and gain adaptation", *Przeglad. Elektrotechniczny.*, vol.89, 2013, 1-6.
- [12] I. Bendaas, F. Naceri, "A new method to minimize the chattering phenomenon in sliding mode control based on intelligent control for induction motor drives", *Serb. J. Electr. Eng.*, vol. 10, June. 2013, 231-246.
- [13] T. Ameid, A. Menacer, H. Talhaoui, and I. Harzelli, "Broken rotor bar fault diagnosis using fast Fourier transform applied to field-oriented control induction machine: simulation and experimental study", *Int. J. Adv. Manuf. Technol.*, 2017.
- [14] Menghal, P. M., Laxmi, A. J., & Anusha, D. (2014), "Speed control of induction motor using fuzzy logic controller", *i-Manager's Journal on Electrical Engineering*, 8(2), 21.
- [15] F. Mokhtari, P. Sicard and A. Hazzab, "Cascade Decentralized Nonlinear PI Control Continuous Production Process", *ELECTRIMACS*, Québec, Canada, Jun. 2008, CD-ROM.
- [16] O. Barambones, P. Alkorta, A. J. Garrido et al. , "An Adaptive Sliding Mode Control Scheme for Induction Motor Drives", *International Journal of Circuit, System and Signal Processing*, vol. 1, no. 1, pp. 73-78, 2007.
- [17] M. Bechar, A. Hazzab, M. Habbab, "Real-Time Scalar Control of Induction Motor using RT-Lab Software", *The 5th International Conference on Electrical Engineering (ICEE-B)*, October. 2017.